Supporting Information

Molecular-scale Study of Cr(VI) Adsorption onto Lepidocrocite Facets by EXAFS, In Situ ATR-FTIR, Theoretical Frequency Calculations and DFT+U Techniques

Xiaofei Li [a], Chuling Guo [*ab], Xiaohu Jin [a], Qian Yao [a], Qianqian Liu [a], Lijuan Zhang [c], Guining Lu [ab], John R. Reinfelder [d], Weilin Huang [d] and Zhi Dang[*ab]

[a] School of Environment and Energy, South China University of Technology, Guangzhou 510006, PR China

[b] The Key Lab of Pollution Control and Ecosystem Restoration in Industry Clusters, Ministry of Education, South China University of Technology, Guangzhou 510006, PR China

[c] School of Chemistry and Chemical Engineering, South China University of Technology, Guangzhou 510006, PR China

[d] Department of Environmental Sciences, Rutgers University, New Brunswick, NJ 08901, USA

19 pages, 4 texts, 12 figures, 9 tables

[*] E-mail: clguo@scut.edu.cn, chzdang@scut.edu.cn; Phone/fax: +86-20-39380508

CONTENTS

Text S1. Modeling Periodic Structure

Lepidocrocite bulk was optimized from the initial structural data[1] using the methods described in the section 2.6.1. After the geometry optimization, to prevent interactions between the surfaces and their periodic images, the corresponding system was then modeled in a supercell geometry with a vacuum of at least 15 Å between the surface slabs. Calculations were conducted on the {010} and {001} lepidocrocite facets. For the {010} periodic model, two lepidocrocite sheets (each one composed by eight atomic layers) were considered for calculation on the {010} lepidocrocite surface.[2] To investigate the variation of surface coverage of adsorbed Cr(VI) complexes, the lateral periodicity is extended to (2 × 2) for the surface of lepidocrocite {010} with respect to models of the clean FeOOH surfaces.[2, 3] In the adsorption study, considering a good compromise between calculation time and the convergence quality, the six first layers of the atoms would be released, which is, and the system was consisted of $Fe_{16}O_{32}H_{16}$ measuring 7.7×6.2×27.1 $Å^3$. For the {001} periodic model, two zigzag sheets were cleaved (1 × 2) as the model of {001} lepidocrocite facet refers to the report of Otte et al.[6] Nine first layers of atoms would be released to conduct the adsorption study, and the system was consisted of $Fe_{16}O_{40}H_{24}$ measuring 6.2×12.5×25.5 $Å^3$. All the systems have considered a dipolar correction to correct for spurious dipolar interactions induced by the use of asymmetric slabs in the supercell approach.[4]

Due to the difficulty in accounting for charged species and surfaces under different solution pH at the water/oxide surface by the DFT calculations in a vacuum. According to the previous study,[2] three types of surfaces, including neutral, hydrated, and deprotonated, were constructed to model different pH situations. In addition, the

surfaces need to be kept neutral due to the known difficulty in dealing charged systems in periodic structures. The “hydrated” surface denoted the acidic conditions, which was modeled by adding a H atom to an OH surface group, whereas the “deprotonated” surface represented the alkaline environment, it could be modeled by eliminating a H atom from an OH surface group.

For Cr(VI) adsorption on the {010} lepidocrocite facet, a total of 13 coordination modes, including monodentate and bidentate complexes, were chosen to investigate appropriate surface structures formed on the {010} LEP facet under different surface coverage and hydrogenation. The effect of surface coverage could be modeled by inserting a second complex on the surface. The influence of pH was modeled by changing the hydrogenation state of surface terminal groups and Cr(VI)-adsorbed species. For the Cr(VI) adsorption configurations on the {001} facet, a total of 14 configurations extended by monodentate and bidentate geometries were tested. The variable conditions could be modeled according to the above description. Therefore, the effects of surface functional groups on the distribution of Cr(VI) species on different lepidocrocite facets could be described by DFT+U methods.

Text S2. Calculations of Cr(VI) adsorption energy

The Cr(VI) adsorption energies were calculated by considering neutral reactants and products under the ligand exchange reaction. For example, the adsorption reaction considered for the substitution of one OH ligand is

$$H_2CrO_4 + (FeO(OH)_n) \rightarrow (CrO_3OH - FeO(OH)_{n-1}) + H_2O \quad (1)$$

The adsorption energy (E_{ads}) of Cr(VI) at lepidocrocite surfaces in [eV/molecule] is described as

$$E_{ads} = \frac{1}{n}(E_{facet-ads} - E_{facet} - nE_{H_2CrO_4}) \quad (2)$$

where n is the initial number of hydroxyl groups on the surface. E_{facet} is the total energy of specific facet; $E_{facet\text{-}ads}$ is the total energy of the specific surfaces with adsorbing Cr(VI). The total energies of isolated species (water, CrO_4H_2, etc.) are selected as the reference energies, which are calculated in a box of 10 × 10 × 10 $Å^3$.[3]

Text S3. Adsorption kinetic and isotherms

The Cr(VI) adsorption processes were well described by using the following Pseudo-second-order kinetic model.

Pseudo-second-order kinetic model

$$\frac{t}{Q_t} = \frac{1}{K_2 Q_e^2} + \frac{t}{Q_e} \quad (1)$$

Where Q_e and Q_t (mg/g) are the amount of adsorbed metals on lepidocrocite at equilibrium and t min, respectively. K_1 is the first order rate constant (1/min). K_2 (g/mg/min) is the rate constant of pseudo-second-order.[5]

The adsorption equilibrium was described by using the following two isotherm models.

Langmuir adsorption isotherm model

$$Q_e = \frac{Q_m K_L C_e}{1 + K_L C_e} \quad (2)$$

where C_e is the equilibrium concentration of Cr(VI) ions (mg/L), Q_e is the amount of Cr(VI) adsorbed per unit surface area of the lepidocrocite nanoarchitectures at equilibrium (mg/m^2), Q_m (mg/m^2) is the maximum adsorption capacity, and K_L (L/mg) is the equilibrium constant.[6]

Freundlich adsorption isotherm model

$$Q_e = K_F C_e^{1/n} \quad (3)$$

where K_F ((mg/m^2)(mg/L)^n) and 1/n are Freundlich constants related to adsorption capacity and adsorption intensity, respectively.[7]

Text S4. Structural characterization of lepidocrocite bulk and facets

The stabilized initial structure of the lepidocrocite bulk and surface were calculated and presented in Fig. S11. The lattice parameters obtained for the lepidocrocite bulk, a= 3.08 Å, b= 12.5 Å, and c= 3.87 Å (Fig. S2a), are in good agreement with the DFT calculation data (a = 3.09 Å, b = 12.54 Å, and c = 3.88 Å) and experimental data (a = 3.08 Å, b = 12.50 Å, and c = 3.87 Å) described in the previous reports.[2] Different possibilities for Cr(VI) coordination modes depend on the orientation of $Fe(O,OH)_6$ octahedra at the iron oxide facets and the surface iron site.[8] {010} is the predominant exposed facet, which presents a 4-fold coordinated Fe2 site (Fig. S2b), providing a μ_2 terminated site for possibly forming a monodentate binuclear (MB) or bidentate mononuclear (BM, ^{2}E) geometry on this facet. Moreover, there are four μ_2 terminated sites at the surface structure of the cell (2×2), and the surface consists of distorted octahedra with long bands (2.12 Å) directed within the bulk and short bands (2.05 Å) toward the surface. The adsorption sites are separated by a small distance of 3.08 Å on the edge of an octahedron and by 3.87 Å between corners of two different octahedra, which is a relatively longer distance than the present edge distances from 2.61 to 2.89 Å and may consequently be a disadvantage for the formation of bidentate mononuclear (BM) complexes.

For the {001} facet structure, which acted as a 5-fold coordinated Fe2 site, the μ_1 terminated sites mainly contributed to the formation of Cr(VI) monodentate mononuclear (MM, ^{1}V) and bidentate binuclear (BB, ^{2}C) adsorption configurations (Fig. S2c). Four μ_1-terminated sites existed on the cell (1×2), and the intersite distances included small distances and long distances of 2.02 and 2.21 Å, respectively. The distances in the <100> direction of the two neighboring octahedra varied from 2.38 to 3.76 Å; however, they were shorter than those in the <010> direction (approximately

6.51 Å). Therefore, the interfacial Cr(VI) adsorption reactions only occurred on the active sites parallel to the <100> direction instead of the <010> direction.

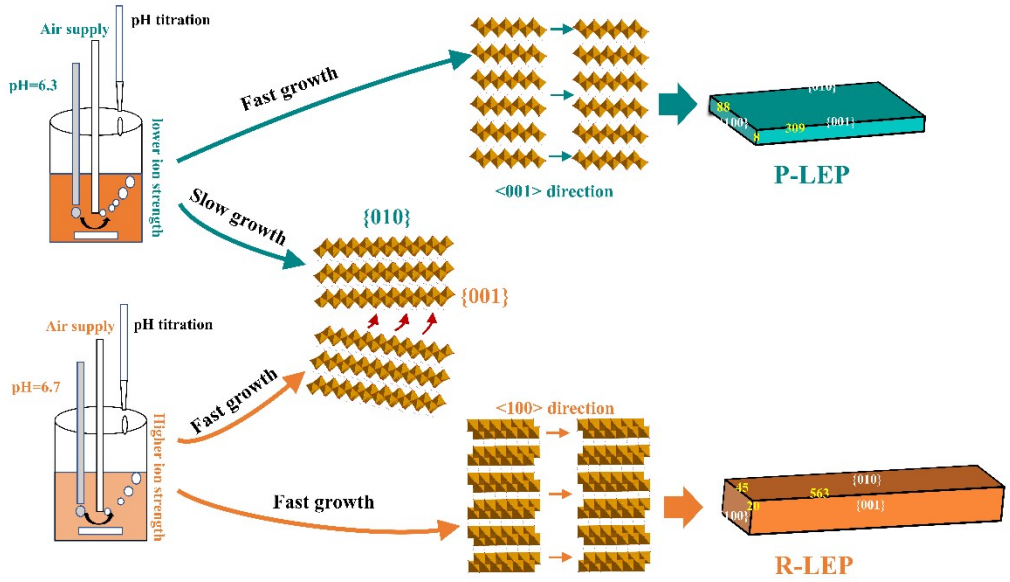

Figure S1. Possible metallogenic processes and facet distributions of P-LEP and R-LEP.

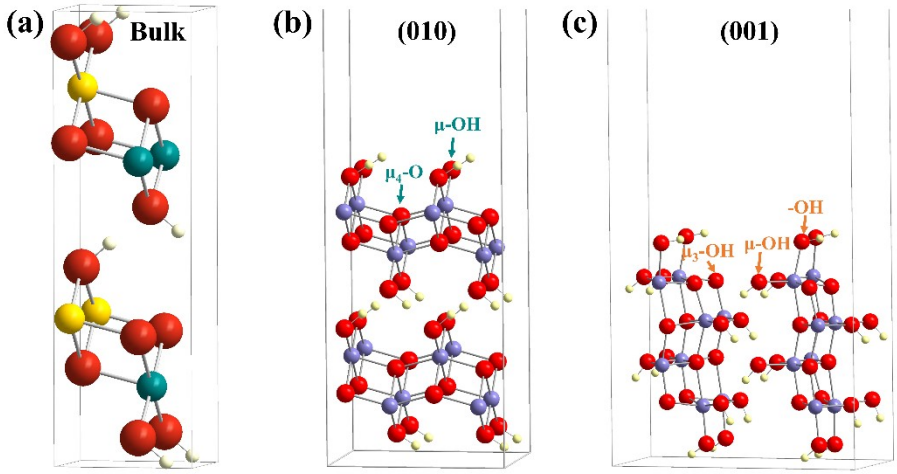

Figure S2. Optimized bulk and surface structure of lepidocrocite, (a) bulk structure in which yellow and dark green spheres represent iron atoms in spin (down) and spin (up) states, respectively, (b) (010) lepidocrocite facet, and (c) (001) lepidocrocite facet. The red spheres, blue spheres and white spheres represent oxygen, iron and hydrogen atoms, respectively.

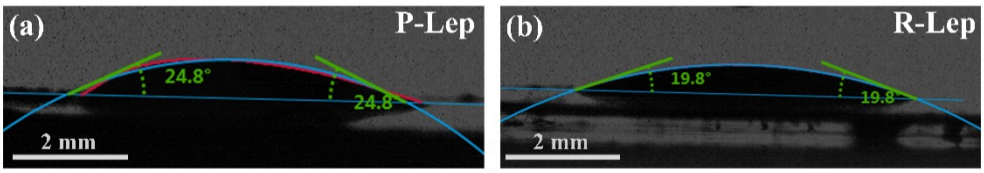

Figure S3. Images of the water droplets on LEP surfaces. (a) P-LEP/H_2O and (b) R-LEP/H_2O.

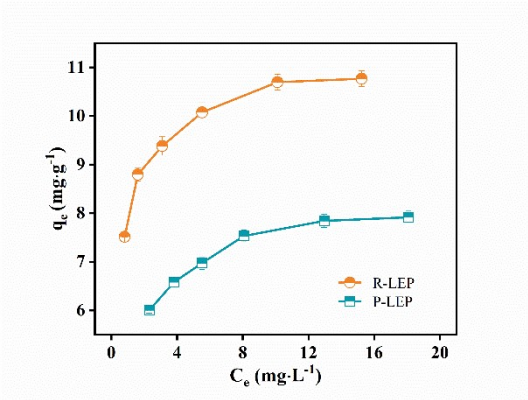

Figure S4. Adsorption isotherm of Cr(VI) on P-LEP and R-LEP. The initial Cr(VI) concentration ranged from 8.32 to 26.0 mg·L^{-1}. The solution pH was 5.0, and the dosage of R-LEP and P-LEP was 1.0 g·L^{-1}. The ionic strength was 0.01 M NaCl.

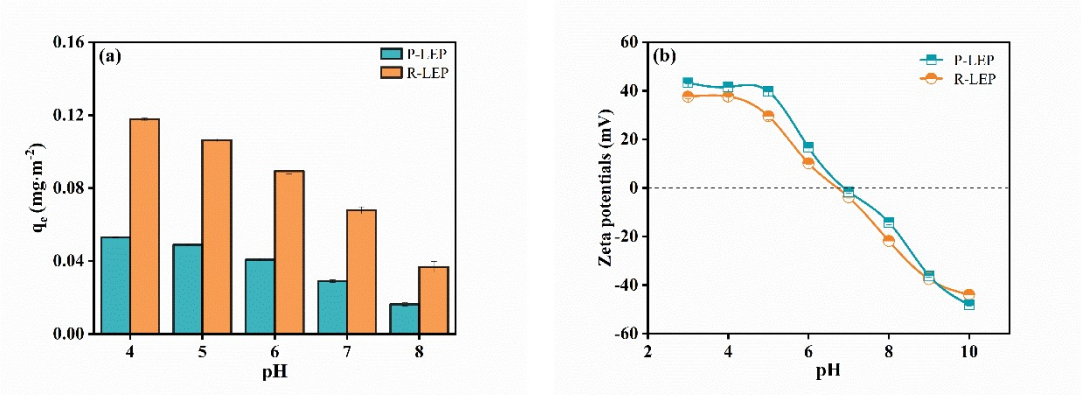

Figure S5. pH adsorption edges for P-LEP and R-LEP (a). The concentrations of Cr(VI) and LEP was 10.4 mg·L^{-1} and 1.0 g·L^{-1}, respectively. The ionic strength was 0.01 M NaCl. The effects of pH on the zeta potential of P-LEP and R-LEP (b).

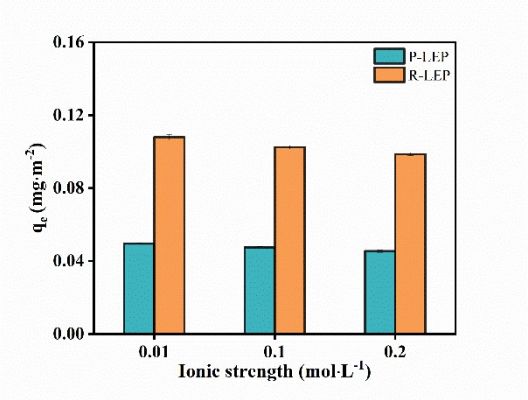

Figure S6. The effects of ionic strength on Cr(VI) adsorption on R-LEP and R-LEP surfaces. The solution pH was 5.0, the concentrations of Cr(VI) and LEP was 10.4 mg·L^{-1} and 1.0 g·L^{-1}, respectively.

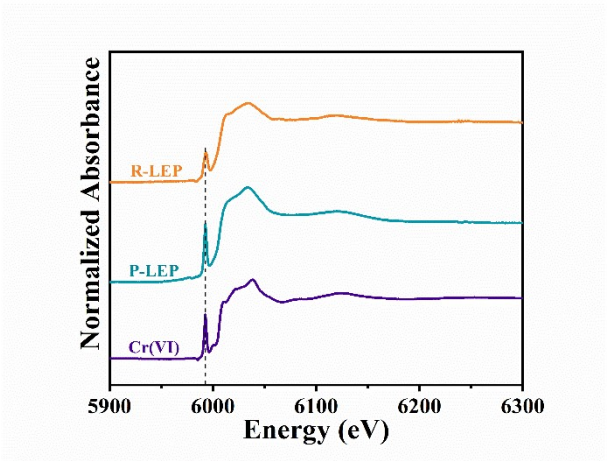

Figure S7. Cr K-edge XANES spectra of adsorbed Cr(VI) on P-LEP and R-LEP, weighted by k^3.

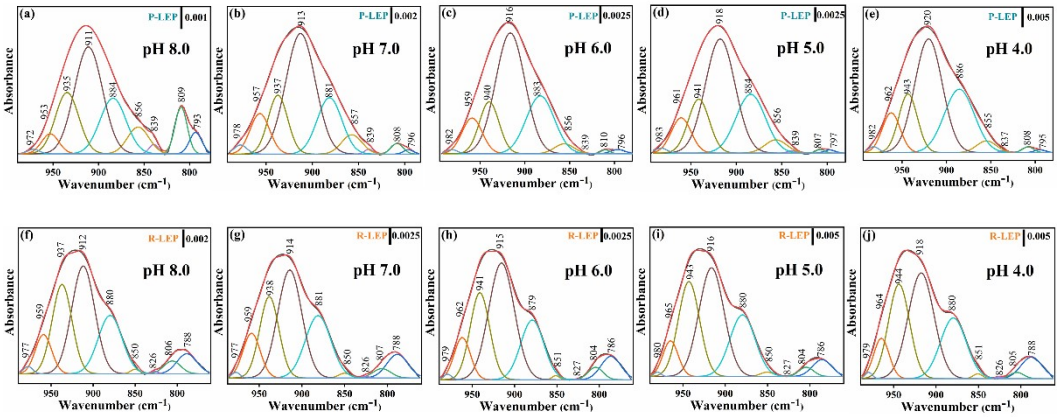

Figure S8. Decomposition spectra of adsorbed Cr(VI) on P-LEP and R-LEP surfaces at pH 8.0, 7.0, 6.0, 5.0, and 4.0 at equilibrium.

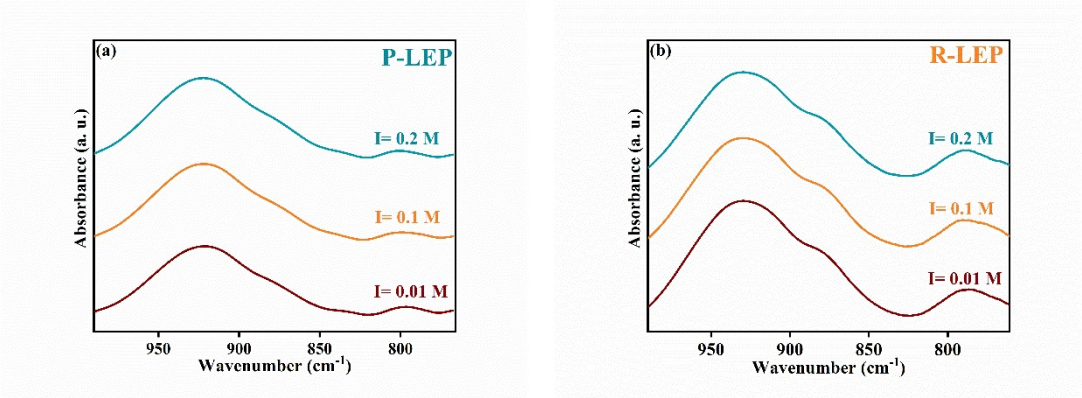

Figure S9. ATR-FTIR spectra of Cr(VI) adsorbed on P-LEP and R-LEP under different ionic strength: 0.01, 0.1, and 0.2 M NaCl. The solution pH was pH 5.0.

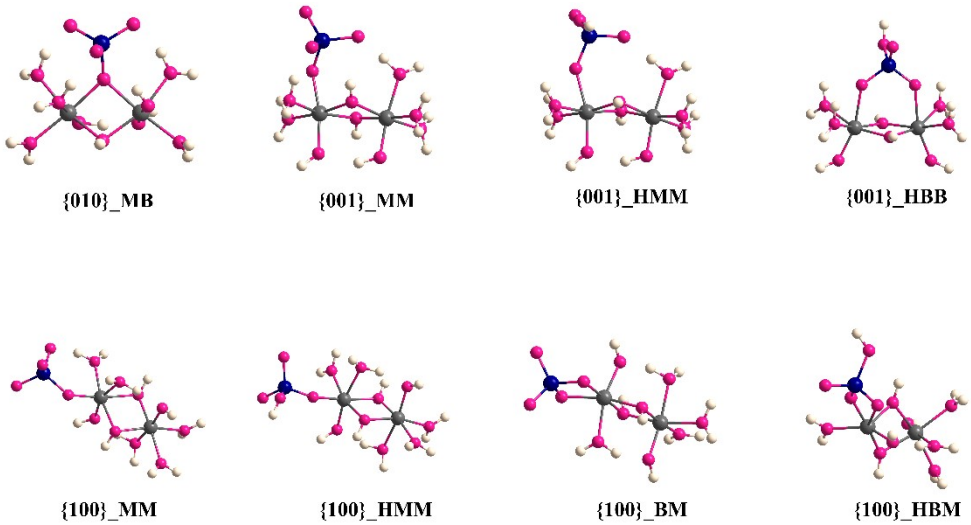

Figure S10. Different optimized adsorption configurations on cluster models extracted from lepidocrocite facets. Monodentate binuclear complexes on {010} facet denoted {010}_MB; nonprotonated and protonated monodentate mononuclear complexes on {001} facet denoted {001}_MM and {001}_HMM, respectively; {001}_HBB: protonated bidentate binuclear complexes on {001} facet; nonprotonated and protonated monodentate mononuclear complexes on {100} facet denoted {100}_MM and {100}_HMM respectively; nonprotonated and protonated bidentate binuclear complexes on {100} facet denoted {100}_BB and {100}_HBB.

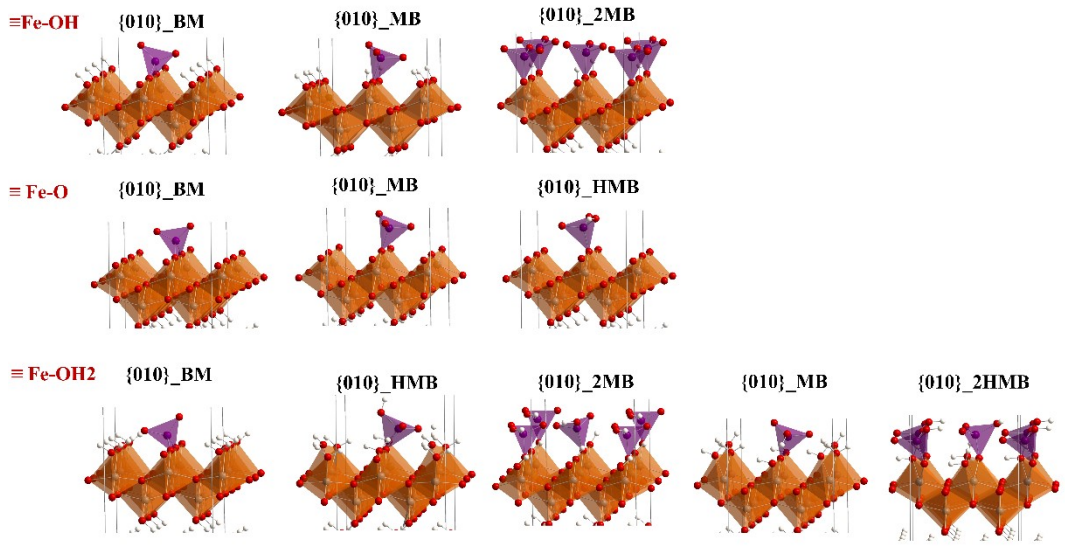

Figure S11. Geometry-optimized periodic models of Cr(VI) adsorbed to {010} lepidocrocite facet. ≡Fe-OH, ≡Fe-O, ≡Fe-OH_2 represented fully hydroxylated neutral surface, fully deprotonated surface, and fully hydrated surface.

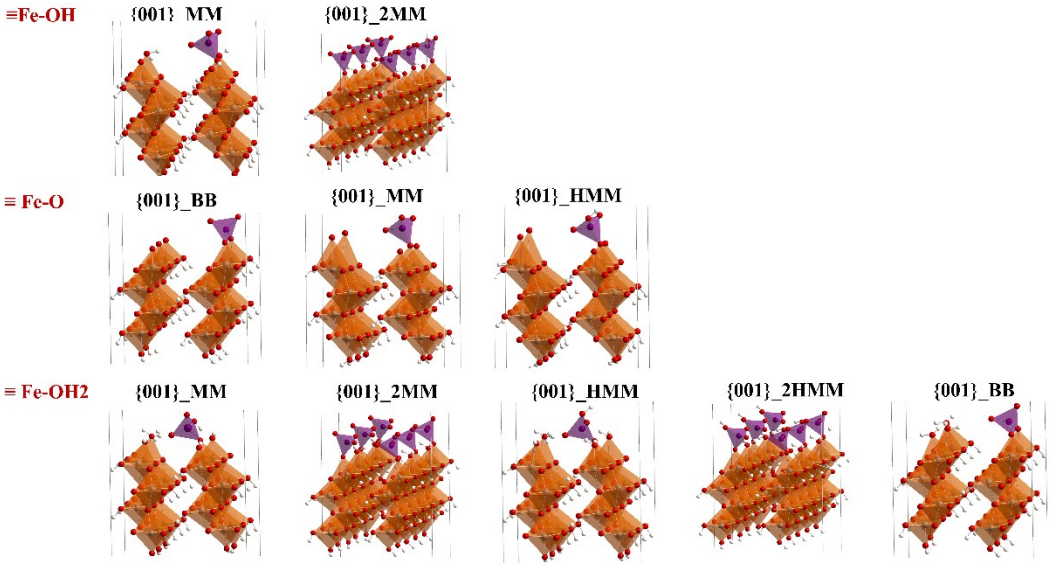

Figure S12. Geometry-optimized periodic models of Cr(VI) adsorbed to {001} lepidocrocite facet. ≡Fe-OH, ≡Fe-O, ≡Fe-OH_2 represented fully hydroxylated neutral surface, fully deprotonated surface, and fully hydrated surface.

Table S1. Kinetics parameters of Cr(VI) adsorption onto P-LEP and R-LEP.

	SSA ($m^2 \cdot g^{-1}$)	q_e ($mg \cdot m^{-2}$)	K_2 ($m^2 \cdot mg^{-1} \cdot min^{-1}$)	K_2 ($g \cdot mg^{-1} \cdot min^{-1}$)	R^2
P-LEP	177	0.045	37.17	0.184	0.9999
R-LEP	61	0.098	31.85	0.455	0.9996

Table S2 Equilibrium adsorption isotherm fitting parameters.

Models	Parameters	P-LEP	R-LEP
Langmuir	q_m ($mg \cdot m^{-2}$)	0.062	0.137
	K_L ($L \cdot mg^{-1}$)	2.60	1.04
	R^2	0.97	0.98
Freundlich	1/n	0.115	0.135
	K_F	0.046	0.090
	R^2	0.94	0.94

Table S3. EXAFS fitting parameters at the Cr K-edge for various samples（S_0^2=0.860）

Sample	Shell	CN^a	R(Å)^b	σ^2(Å^2)^c	ΔE_0(eV)^d	R factor
P-LEP	Cr-O	4	1.68	0.003	-7.7	0.014
	Cr-O-O	12	2.50			
	Cr-Fe1	1.7	3.23			
	Cr-Fe2	0.6	3.60			
R-LEP	Cr-O	4	1.67	0.006	-7.9	0.009
	Cr-O-O	12	2.50			
	Cr-Fe1	1.8	3.15			
	Cr-Fe2	0.4	3.60			

[a]*CN*, coordination number; [b]*R*, distance between absorber and backscatter atoms; [c]σ^2, Debye-Waller factor to account for both thermal and structural disorders; [d]ΔE_0, inner potential correction; *R* factor indicates the goodness of the fit. $S0^2$ was fixed to 0.860, according to the experimental EXAFS fit of Cr foil by fixing CN as the known crystallographic value. Fitting range: $2.0 \leq k$ (/Å) $\leq$ ~10 and $1 \leq R$ (Å) ≤ 3.5 (PLEP); $2.0 \leq k$ (/Å) ≤ 10 and $1.0 \leq R$ (Å) ≤ 3.5 (RLEP). A reasonable range of EXAFS fitting parameters: $0.700 < S_0^2 < 1.000$; $CN > 0$; $\sigma^2 > 0$ Å^2; $\Delta E_0 < 10$ eV; *R* factor < 0.02.

Table S4. Calculated Cr–O Stretching Frequencies (cm^{-1}) of Chromate-Iron Oxide Clusters (UB3LYP/LANL2DZ)

States	$MB_{\{010\}}$	$MM_{\{001\}}$	$BB_{\{001\}}$	$MM_{\{100\}}$	$BM_{\{100\}}$
Non-protonated	942	960	952	952	969
	915	894	929	943	948
	894	869	834	933	939
	875	827	807	866	797
Protonated	989	996	970	1000	1003
	956	943	890	974	964
	886	908	874	944	940
	845	886	831	863	838

Table S5. Reactions considered for the adsorption energy calculations and corresponding values obtained for Cr(VI) adsorption on lepidocrocite {010} facet in the gas phase. The most stable configurations considered in the article are given in bold letters. The total energies of isolated species (water, H_2CrO_4 …) needed as reference energies, are calculated in a box of 10×10×10 $Å^3$.

System	**Modes**	**Energetic calculations**	**E_{ads} (eV)**
OH	MB	$(E_{s\text{-}a}+0.5E_{H2}+E_{H2O})-(E_s+E_{H2CrO4})$	1.54
	HMB	$(E_{s\text{-}a}+E_{H2O})-(E_s+E_{H2CrO4})$	**-0.35**
	2MB	$0.5[(E_{s\text{-}a}+E_{H2}+2E_{H2O})-(E_s+2E_{H2CrO4})]$	2.16
	2HMB	$0.5[(E_{s\text{-}a}+2E_{H2O})-(E_s+2_{EH2CrO4})]$	**-0.32**
	BM	$(E_{s\text{-}a}+2E_{H2O})-(E_s+E_{H2CrO4})$	0.61
O	MB	$(E_{s\text{-}a}+2E_{H2}+E_{H2O})-(E_s+E_{H2CrO4})$	9.62
	HMB	$(E_{s\text{-}a}+1.5E_{H2}+E_{H2O})-(E_s+E_{H2CrO4})$	6.73
	BM	$(E_{s\text{-}a}+E_{H2}+2E_{H2O})-(E_s+E_{H2CrO4})$	5.49
OH2	MB	$(E_{s\text{-}a}+0.5E_{O2})-(E_s+E_{H2CrO4})$	1.52
	HMB	$(E_{s\text{-}a}+0.5E_{O2})-(E_s+E_{H2CrO4}+0.5E_{H2})$	0.65
	2MB	$0.5[(E_{s\text{-}a}+E_{O2}+2E_{H2})-(E_s+2E_{H2CrO4})]$	2.84
	2HMB	$0.5[(E_{s\text{-}a}+E_{O2}+E_{H2})-(E_s+2E_{H2CrO4})]$	1.99
	BM	$(E_{s\text{-}a}+0.5E_{O2}+E_{H2O})-(E_s+E_{H2CrO4})$	1.69

MB, BM, HMB were denoted as monodentate binuclear, bidentate mononuclear, and protonated monodentate binuclear.

Table S6. Reactions considered for the adsorption energy calculations and corresponding values obtained for Cr(VI) adsorption on lepidocrocite {001} facet in the gas phase. The most stable configurations considered in the article are given in bold letters. The total energies of isolated species (water, H_2CrO_4 …) needed as reference energies, are calculated in a box of 10×10×10 $Å^3$.

System	Modes	Energetic calculations	E_{ads} (eV)
OH	MM	$(E_{s-a}+0.5E_{H2}+E_{H2O})-(E_s+E_{H2CrO4})$	1.88
	HMM	$(E_{s-a}+E_{H2O})-(E_s+E_{H2CrO4})$	**-0.35**
	2MM	$0.5[(E_{s-a}+E_{H2}+2E_{H2O})-(E_s+2E_{H2CrO4})]$	2.33
	2HMM	$0.5[(E_{s-a}+2E_{H2O})-(E_s+2_{EH2CrO4})]$	**-0.32**
	BB	$(E_{s-a}+2E_{H2O})-(E_s+E_{H2CrO4})$	**-0.61**
	2BB	$0.5(E_{s-a}+4E_{H2O})-(E_s+2E_{H2CrO4})$	**-0.15**
O	MM	$(E_{s-a}+2E_{H2}+E_{H2O})-(E_s+E_{H2CrO4})$	6.02
	HMM	$(E_{s-a}+1.5E_{H2}+E_{H2O})-(E_s+E_{H2CrO4})$	3.70
	BB	$(E_{s-a}+E_{H2}+2E_{H2O})-(E_s+E_{H2CrO4})$	4.41
OH_2	MM	$(E_{s-a}+0.5E_{O2})-(E_s+E_{H2CrO4})$	-22.36
	HMM	$(E_{s-a}+0.5E_{O2})-(E_s+E_{H2CrO4}+0.5E_{H2})$	-23.90
	2MM	$0.5[(E_{s-a}+E_{O2}+2E_{H2})-(E_s+2E_{H2CrO4})]$	2.54
	2HMM	$0.5[(E_{s-a}+E_{O2}+E_{H2})-(E_s+2E_{H2CrO4})]$	-0.02
	BB	$(E_{s-a}+0.5E_{O2}+E_{H2O})-(E_s+E_{H2CrO4})$	-2.43

MM, BB, and HMM were denoted as monodentate mononuclear, bidentate binuclear, and protonated monodentate mononuclear.

Table S7. Comparison of different reactions energies considered at the neutral (OH terminated) {010} and {001} facets, taking into account the product (H_2O) solvation free energy.

System	N_H[a]	N_{H2O}[b]	$E_{gas-ads}$[c](eV)	$E_{Liq-ads}$[d](eV)	$\Delta\Delta E_{liq}$[e](eV)
{010} Facet					
HMB	0	1	-0.35	-0.80	0
MB	0	2	0.61	-0.29	0.51
2HMB	0	1	-0.32	-0.77	0.03
{001} Facet					
HMM	0	1	-0.35	-0.80	0
BB	0	2	-0.61	-1.51	-0.71
2HMM	0	1	-0.32	-0.77	0.03
2BB	0	2	-0.15	-1.05	-0.25

[a] denotes the number of protons released; [b] Number of water molecules released; [c] Gas phase reaction; [d] means that the $E_{Liq-ads} = E_{gas-ads} - 0.45n$, and the "n" denoted the number of water; e means the difference in adsorption energy from the liquid phase between the two coordination modes.

Table S8. Structural parameters of Cr(VI) adsorption configurations on {010} lepidocrocite facet.

Terminated Groups	Modes	d_{Fe-Cr} (Å)	d_{Fe-O} (Å)	d_{Cr-O} (Å)	$\angle_{Fe-O-Cr}$ (°)
OH	MB	3.40/3.42	1.97/1.99	1.82	127.25/127.51
	HMB	3.48/3.49	2.14/2.11	1.71	130.48/131.06
	2HMB	3.44/3.52	2.06/2.08	1.75	127.80/134.63
	BM	2.68	2.09/2.10	1.75/1.75	88.11/87.91
O	MB	3.40/3.47	2.00/2.05	1.80	126.72/128.21
	HMB	3.45/3.45	2.01/2.08	1.78	126.34/130.73
	BM	2.67	2.06/2.06	1.79	87.63/87.73
OH_2	MB	3.45/3.50	2.12/2.14	1.70	128.83/131.19
	HMB	3.35/3.42	2.05/2.11	1.76	119.75/129.43
	2MB	3.46/3.51/3.51	2.07/2.07/2.09/2.10	1.74/1.75	129.44/130.89
					130.98/133.25
	2HMB	3.68/3.57	2.17/2.19/2.23/2.24	1.71/1.72	120.71/133.98
		3.40/3.58			129.55/138.47
	BM	2.76	2.18/2.19	1.70	89.92/89.59

Table S9. Structural parameters of Cr(VI) adsorption configurations on {001} lepidocrocite facet.

Terminated Groups	Modes	d_{Fe-Cr} (Å)	d_{Fe-O} (Å)	d_{Cr-O} (Å)	$\angle_{Fe-O-Cr}$ (°)
-*OH*	MM	3.40	1.87	1.72	141.35
	HMM	3.42	1.88	1.72	143.14
	2MM	3.52/3.56	1.84/1.86	1.71/1.72	163.61/173.36
	2HMM	3.56/3.57	1.84/1.86	1.71/1.73	173.25/174.49
	BB	3.29/3.30	1.93/1.94	1.69/1.70	131.07/129.87
	2BB	3.28/3.32	1.91/1.95	1.69/1.71	130.43/131.27
-*O*	MM	3.41	1.86	1.72	144.11
	HMM	3.39	1.87	1.73	140.62
	BB	3.30/3.31	1.94/1.95	1.69/1.70	130.81/130.20
-OH_2	MM	3.42	1.97	1.70	136.92
	HMM	3.61	2.20	1.65	139.27
	2MM	3.49/3.52	1.91/1.96	1.69/1.72	146.16/150.54
	2HMM	3.53/3.55	1.96/1.97	1.67/1.72	149.77/150.98
	BB	3.22	1.88//1.91	1.72/1.73	125.08/125.91

References

(1) A.N. Christensen, M.S. Lehmann, P. Convert, L. Beyer, S.J. Cyvin, Deuteration of Crystalline Hydroxides. Hydrogen Bonds of gamma-AlOO(H,D) and gamma-FeOO(H,D). Acta. Chem. Scand, 1982, 36, 303-308.

(2) A. Davantès, D. Costa, G. Lefèvre, Molybdenum(VI) Adsorption onto Lepidocrocite (γ-FeOOH): In Situ Vibrational Spectroscopy and DFT+U Theoretical Study. J. Phys. Chem. C, 2016, 120, 11871-11881.

(3) K. Otte, W.W. Schmahl, R. Pentcheva, DFT+U Study of Arsenate Adsorption on FeOOH Surfaces: Evidence for Competing Binding Mechanisms. J. Phys. Chem. C, 2013, 117, 15571-15582.

(4) D. Tunega, Theoretical Study of Properties of Goethite (α-FeOOH) at Ambient and High-Pressure Conditions. J. Phys. Chem. C, 2012, 116, 6703–6713.

(5)Y.S. Ho, G. Mckay, Pseudo-second order model for sorption processes. Process Biochem., 1999, 34, 451-465.

(6) I. Langmuir, The constitution and fundamental properties of solids and liquids. Part 1. Solids. J. Am. Chem. Soc, 1917, 38, 2221-2295.

(7) H. Freundlich, Scientific Books: Colloid and Capillary Chemistry. Science, 1927, 65, 40-41.

(8) S. Yin, D.E. Ellis, DFT studies of Cr(VI) complex adsorption on hydroxylated hematite surfaces, Surf. Sci., 603 (2009) 736-746.